

Citation for published version:
Burton, LA & Walsh, A 2013, 'Band alignment in SnS thin-film solar cells: Possible origin of the low conversion efficiency', Applied Physics Letters, vol. 102, no. 13, 132111. https://doi.org/10.1063/1.4801313

DOI: 10.1063/1.4801313

Publication date: 2013

Document Version Publisher's PDF, also known as Version of record

Link to publication

Copyright 2013 American Institute of Physics. This article may be downloaded for personal use only. Any other use requires prior permission of the author and the American Institute of Physics.

The following article appeared in Burton, LA & Walsh, A 2013, 'Band alignment in SnS thin-film solar cells: Possible origin of the low conversion efficiency' Applied Physics Letters, vol 102, no. 13, 132111 and may be found at http://link.aip.org/link/doi/10.1063/1.4801313

## **University of Bath**

## **Alternative formats**

If you require this document in an alternative format, please contact: openaccess@bath.ac.uk

Copyright and moral rights for the publications made accessible in the public portal are retained by the authors and/or other copyright owners and it is a condition of accessing publications that users recognise and abide by the legal requirements associated with these rights.

**Take down policy**If you believe that this document breaches copyright please contact us providing details, and we will remove access to the work immediately and investigate your claim.

Download date: 09 Mar 2023



## Band alignment in SnS thin-film solar cells: Possible origin of the low conversion efficiency

Lee A. Burton and Aron Walsh<sup>a)</sup>

Centre for Sustainable Chemical Technologies and Department of Chemistry, University of Bath, Claverton Down, Bath BA2 7AY, United Kingdom

(Received 25 January 2013; accepted 26 March 2013; published online 4 April 2013)

Tin sulfide is an attractive absorber material for low-cost thin-film solar cells. Despite the ideal physical properties of bulk SnS, the photovoltaic conversion efficiencies achieved in devices to date have been no greater than 2%. Assessment of the valence band energy of the stable orthorhombic phase of SnS reveals a low ionisation potential (4.7 eV) in comparison to typical absorber materials (CdTe, CuInSe<sub>2</sub>, and Cu<sub>2</sub>ZnSnS<sub>4</sub>). A band mis-alignment is therefore predicted with commonly used back contact and buffer layers. Alternative configurations are proposed that should improve device performance. © 2013 AIP Publishing LLC. [http://dx.doi.org/10.1063/1.4801313]

The two main light-absorbing materials used in thin-film photovoltaics are CdTe and Cu(In,Ga)(S,Se)<sub>2</sub> (CIGS), the latter of which has recently achieved a record solar conversion efficiency of 20.3%. However, the expense and scarcity of In, Ga, and Te and the environmental toxicity of Cd have motivated the search for materials better suited for sustainable, large-scale production. <sup>2</sup>

One of the most intensively studied next-generation materials is Cu<sub>2</sub>ZnSnS<sub>4</sub> (CZTS),<sup>3,4</sup> although the binary compound SnS should in principle be more straightforward to produce and optimise than a quaternary system. While SnS combines the set of materials characteristics suitable for high-performance photovoltaics (an optical band gap of 1.3 eV; high light absorption coefficient; 6-8 robust p-type conductivity; good carrier mobility), the performance of SnS solar cells has only recently reached 2% conversion efficiency. 11 The low performance could initially be blamed on poor film quality, i.e., polycrystalline films with the presence of multiple secondary phases. In particular, at least three stoichiometries (SnS, Sn<sub>2</sub>S<sub>3</sub>, and SnS<sub>2</sub>) are known to exist.<sup>12</sup> However, the recent application of atomic layer and chemical vapour deposition (ALD/CVD) techniques has succeeded in producing high-quality phase pure films, 10,13 without a significant increase in efficiency, while device analysis shows the high current density and low voltage characteristic of poor band alignment. 11

In this Letter, we demonstrate that, based on electronic structure calculations using a hybrid non-local density functional, the extremely low ionisation potential of SnS produces a band mis-alignment of ca. 1 eV with the absorber materials commonly used in thin-film photovoltaic devices. Based on the predicted valence band energy of SnS, we propose a number of buffer and contact layers that should result in improved photovoltaic conversion efficiencies.

The ground-state orthorhombic crystal structure (space group *Pnma*)<sup>14</sup> of SnS was first calculated using density functional theory (DFT), with the exchange-correlation functional of Perdew, Burke, and Ernzerhof revised for solids (PBEsol).<sup>15</sup> The structural parameters were held fixed at the experimentally determined values to avoid errors due to van

The (100) surface model for SnS and the associated electrostatic potential (from the HSE06 calculations) are shown in Figure 1. The value of the electrostatic potential at the plateau is used as reference energy with which to align the valence band of SnS. The associated surface ionisation

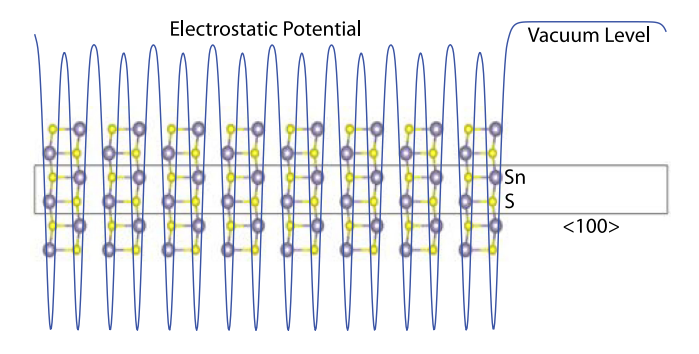


FIG. 1. Structure of the 8-bilayer 2D slab model and the corresponding electrostatic (Hartree) potential at the HSE06 level of theory, which is used to align the electronic eigenvalues to the vacuum level.

der Waals interactions, which are small but not negligible for this pseudo-layered structure. To align the electronic band energies to the vacuum level, a surface slab model (15 Å vacuum spacing) was constructed. The (100) surface of SnS was chosen as it is a non-polar termination that results in minimal bond cleavage, and does not produce any undesirable surface states. We followed a three-step computational procedure: (i) surface structure generation and calculation at the semi-local PBEsol level of theory; (ii) electronic structure optimisation using a non-local hybrid exchange-correlation functional developed by Heyd, Scuseria, and Ernzerhof (HSE06); 16 and (iii) calculation of the quasiparticle energies using a perturbative  $G_0W_0$  approach. The slab thickness was rigorously checked for convergence with respect to the vacuum potential. All calculations were performed using the VASP code, <sup>19</sup> with the projector augmented wave (PAW) approach, <sup>20</sup> a 400 eV plane wave cut-off, and reciprocal space sampling of 4 × 6  $\times$  6 k-points (1  $\times$  6  $\times$  6 k-points for the 2D slab). Parallelism across k-points was performed to utilise 512 computing cores.<sup>21</sup> The  $G_0W_0$  calculations included 512 bands, 80 of which were occupied, and local field effects in the exchangecorrelation potential were also treated.

<sup>&</sup>lt;sup>a)</sup>Electronic mail: a.walsh@bath.ac.uk

potential is calculated to be  $-4.67 \,\mathrm{eV}$ ,  $-4.69 \,\mathrm{eV}$ , and  $-4.70 \,\mathrm{eV}$  for 2, 4, and 8 atomic bilayers, respectively. The 8-bilayer slab is fully converged. The contribution of the surface to the calculated ionisation potential is small: when the vacuum level is aligned to the bulk eigenvalues, through core level eigenvalues in the centre of the slab, the ionisation potential is not modified, to within  $0.02 \,\mathrm{eV}$ . SnS is a p-type semiconductor; hence, the equilibrium Fermi level will be placed close to the valence band edge, and the workfunction and the ionisation potential should be close in energy. A previous photoemission measurement placed the workfunction at  $4.2 \,\mathrm{eV}$  below the vacuum level for a (001) terminated single crystal; however, the Fermi level was reported near the conduction band, which for p-type SnS suggests significant surface band bending (electron accumulation).

Values of the ionisation potential calculated at the HSE06 level of theory are approximately 0.2 eV larger than for PBEsol, which is expected due to the reduction in selfinteraction with the addition of exact electron-exchange. Calculations performed using perturbative  $G_0W_0$  based on the HSE06 wavefunctions were found to result in a decrease in the ionisation potential by 0.8 eV. The immense computational expense makes it impossible to assess the importance, for surfaces, of self-consistency or vertex corrections in the many-body GW formalism; however, a similar shift is also observed for the bulk electron energies of SnS (to within 0.05 eV). While recent studies have shown that the band edge positions of sp-bonded materials are comparable in hybrid-DFT and GW calculations, systems containing shallow core or valence d-bands display significant deviations.<sup>23,24</sup> It should be noted that the electronic configuration found in SnS is a special case  $(Sn^{II}:4d^{10}5s^{2}5p^{0})$ . At this time, the HSE06 functional appears to offer the best compromise between accuracy and efficiency; the magnitude of the calculated band gap suggests an uncertainty in the electron energies of the order of 0.1 eV.

The predicted ionisation potential of SnS is lower than that typically found for metal-chalcogenide semiconductors, 25 which can be explained by the unusual coordination environment, and level repulsion, caused by low binding energy Sn 5s<sup>2</sup> orbitals. The crystal structure is an elongation of rocksalt, where the octahedral cation environment is distorted to give three short (ca. 2.6 Å) and three long (ca. 3.2 Å) Sn-S bonds due to the stereochemically active lone pair.<sup>26</sup> In this lower oxidation state of Sn (i.e., II), the 5s<sup>2</sup> orbitals are formally occupied, with the conduction band formed from the empty 5p band.<sup>26</sup> The interaction of Sn 5s and S 3p results in antibonding states at the top of the valence band.<sup>27</sup> In contrast, the ionisation potentials of CdTe and CuInSe<sub>2</sub> have been reported as 5.7 eV from ultraviolet photoelectron spectroscopy<sup>28</sup> and HSE06 calculations, respectively.<sup>29</sup> These values are also close to those found for CZTS and related selenide materials.<sup>3</sup>

The majority of SnS solar cells produced to date have been based on adopting the architecture developed for CdTe and CIGS, where SnS is deposited on Mo-coated glass and covered with an n-type buffer layer of CdS. The band alignment of SnS with these materials is shown in Figure 2 based upon our predicted ionisation potential, the fundamental (indirect) band gap of ca. 1.1 eV, <sup>30,31</sup> and literature values. <sup>3,28,29,32</sup> It is apparent that the valence band and

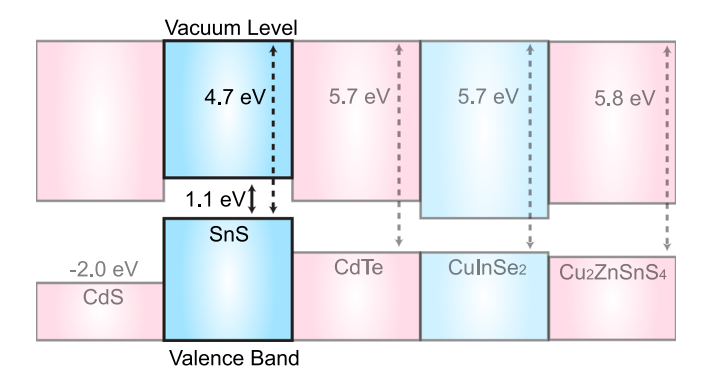


FIG. 2. Predicted band alignment between SnS (HSE06 ionisation potential) and a range of materials used in thin-film solar cells from Refs. 3, 28, 29, and 32.

TABLE I. Candidate electrical contacts for SnS devices based on energy level alignment and element availability. Values for metals are taken from Ref. 33 and values for semiconductor buffers from Refs. 34 and 35.

Metallic contacts	Workfunction (eV)	n-type buffers	Workfunction <sup>a</sup> (eV)
Titanium	4.33	(Zn,Cd)S	2.95 (ZnS) – 3.88 (CdS)
Tungsten	4.55	Zn(S,Se)	2.95 (ZnS) – 4.09 (ZnSe)
Tin	4.42	Zn(O,S)	3.91 (ZnO) – 2.95 (ZnS)

<sup>a</sup>Equated to reported electron affinities/conduction band edge due to n-type nature. The limiting energies for the semiconductor solid-solutions are taken as those of the parent binary compounds. It should be noted that absolute values can vary according to the particular sample and/or study.

conduction bands of SnS are misaligned, with the valence band energy of SnS equalling the conduction band energy of CuInSe<sub>2</sub> and approaching the conduction band energy of CdS. New device configurations are required to be suitable for SnS. For the transport of photo-generated holes, a material with a lower workfunction than Mo may be optimal, while for the buffer layer, a material with a higher conduction band (smaller electron affinity) than CdS will be required. We report a number of candidate materials for tin sulfide device contacts, based on energy level alignment and elemental availability in Table I. Indeed the potential for the Zn(O,S) solid-solution has very recently been demonstrated.<sup>11</sup>

It should be noted that our analysis is based on the natural band alignments, i.e., discounting any effect of interfacial strain, electrostatic dipoles, or chemical interactions that may significantly change the nature of the microscopic energy levels. For example, the reaction between Mo and S has recently been observed to occur in CZTS solar cells, and a similar interaction could explain the complex temperature dependence observed for SnS Ohmic contacts. The effects of band bending at semiconductor interfaces are well documented, but are beyond the scope of the present study.

In summary, we have evaluated the electron energies of SnS and analysed them with respect to its application in thinfilm solar cells. A deficiency in the commonly used architecture is identified and routes to overcome it is proposed. Further investigation of this system is warranted.

We thank Gilles Dennler for useful discussions and acknowledge membership of the UK's HPC Materials Chemistry Consortium, which was funded by EPSRC grant EP/F067496. A.W. acknowledges support from the Royal Society for a University Research Fellowship, and L.A.B was funded by EPSRC (Grant No. EP/G03768X/1).

- <sup>1</sup>P. Jackson, D. Hariskos, E. Lotter, S. Paetel, R. Wuerz, R. Menner, W. Wischmann, and M. Powalla, Prog. Photovolt. **19**, 894 (2011).
- <sup>2</sup>L. M. Peter, Philos. Trans. R. Soc. A **369**, 1840 (2011).
- <sup>3</sup>A. Walsh, S. Chen, S. H. Wei, and X. G. Gong, Adv. Energy Mater. **2**, 400 (2012).
- <sup>4</sup>T. K. Todorov, K. B. Reuter, and D. B. Mitzi, Adv. Mater. **22**, E156 (2010). <sup>5</sup>M. Parenteau and C. Carlone, Phys. Rev. B **41**, 5227 (1990).
- <sup>6</sup>K. R. Reddy, N. K. Reddy, and R. Miles, Sol. Energy Mater. Sol. C. **90**, 3041 (2006).
- <sup>7</sup>M. Devika, K. T. R. Reddy, N. K. Reddy, K. Ramesh, R. Ganesan, E. S. R. Gopal, and K. R. Gunasekhar, J. Appl. Phys. **100**, 023518 (2006).
- <sup>8</sup>C. S. Ferekides, U. Balasubramanian, R. Mamazza, V. Viswanathan, H. Zhao, and D. L. Morel, Sol. Energy 77, 823 (2004).
- <sup>9</sup>E. Guneri, F. Gode, C. Ulutas, F. Kirmizigul, G. Altindemir, and C. Gumus, Chalcogenide Lett. **7**, 685 (2010).
- <sup>10</sup>P. Sinsermsuksakul, J. Heo, W. Noh, A. S. Hock, and R. G. Gordon, Adv. Energy Mater. 1, 1116 (2011).
- <sup>11</sup>P. Sinsermsuksakul, K. Hartman, S. B. Kim, J. Heo, L. Sun, H. H. Park, R. Chakraborty, T. Buonassisi, and R. G. Gordon, Appl. Phys. Lett. 102, 053901 (2013).
- <sup>12</sup>L. A. Burton and A. Walsh, J. Phys. Chem. C **116**, 24262 (2012).
- <sup>13</sup>P. Sinsermsuksakul, R. Chakraborty, S. B. Kim, S. M. Heald, T. Buonassisi, and R. G. Gordon, Chem. Mater. 24, 4556 (2012).
- <sup>14</sup>T. Chattopadhyay, J. Pannetier, and H. G. Von Schnering, J. Phys. Chem. Solids 47, 879 (1986).
- J. P. Perdew, A. Ruzsinszky, G. I. Csonka, O. A. Vydrov, G. E. Scuseria, L. A. Constantin, X. Zhou, and K. Burke, Phys. Rev. Lett. 100, 136406 (2008).
   Heyd, G. E. Scuseria, and M. Ernzerhof, J. Chem. Phys. 124, 219906 (2006).

- <sup>17</sup>L. Hedin, Phys. Rev. **139**, A796 (1965).
- <sup>18</sup>M. Shishkin and G. Kresse, Phys. Rev. B **75**, 235102 (2007).
- <sup>19</sup>G. Kresse and J. Furthmüller, Phys. Rev. B **54**, 11169 (1996).
- <sup>20</sup>G. Kresse and D. Joubert, Phys. Rev. B **59**, 1758 (1999).
- <sup>21</sup>A. Maniopoulou, E. R. M. Davidson, R. Grau-Crespo, A. Walsh, I. J. Bush, C. R. A. Catlow, and S. M. Woodley, Comput. Phys. Commun. 183, 1696 (2012).
- <sup>22</sup>A. R. H. F. Ettema, R. A. de Groot, C. Haas, and T. S. Turner, Phys. Rev. B 46, 7363 (1992).
- <sup>23</sup>W. Chen and A. Pasquarello, Phys. Rev. B **86**, 035134 (2012).
- <sup>24</sup>S. Lany, Phys. Rev. B **87**, 085112 (2013).
- <sup>25</sup>B. R. K. Ellmer and K. Andreas, *Transparent Conductive Zinc Oxide* (Springer-Verlag, 2008).
- <sup>26</sup>L. A. Burton and A. Walsh, J. Solid State Chem. **196**, 157 (2012).
- <sup>27</sup>A. Walsh, D. J. Payne, R. G. Egdell, and G. W. Watson, Chem. Soc. Rev. 40, 4455 (2011).
- <sup>28</sup>G. Teeter, J. Appl. Phys. **102**, 034504 (2007).
- <sup>29</sup>Y. Hinuma, F. Oba, Y. Kumagai, and I. Tanaka, Phys. Rev. B 86, 245433 (2012).
- <sup>30</sup>J. Vidal, S. Lany, M. d'Avezac, A. Zunger, A. Zakutayev, J. Francis, and J. Tate, Appl. Phys. Lett. **100**, 032104 (2012).
- <sup>31</sup>W. Albers, C. Haas, H. J. Vink, and J. D. Wasscher, J. Appl. Phys. 32, 2220 (1961).
- <sup>32</sup>Y. Li, A. Walsh, S. Chen, W. Yin, J. Yang, J. Li, J. Da Silva, X. Gong, and S. Wei, Appl. Phys. Lett. **94**, 212109 (2009).
- <sup>33</sup>CRC Handbook of Chemistry and Physics, 92nd ed. (CRC Press, Boca Raton, FL, 2011–2012).
- <sup>34</sup>Y. Xu and M. A. A. Schoonen, Am. Minerol. **85**, 543 (2000).
- <sup>35</sup>R. K. Swank, Phys. Rev. **153**, 844 (1967).
- <sup>36</sup>Z. Zhang and J. T. Yates, Chem. Rev. **112**, 5520 (2012).
- <sup>37</sup>J. J. Scragg, J. T. Watjen, M. Edoff, T. Ericson, T. Kubart, and C. Platzer-Bjorkman, J. Am. Chem. Soc. 134, 19330 (2012).
- <sup>38</sup>M. Devika, N. K. Reddy, F. Patolsky, and K. R. Gunasekhar, J. Appl. Phys. **104**, 124503 (2008).